EUROPEAN ORGANIZATION FOR NUCLEAR RESEARCH

Proposal to the ISOLDE and Neutron Time-of-Flight Committee

Production of phosphorus-vacancy centers in diamond for optical and spin characterization

Submitted 2018-01-10

B. L. Green[1], M. E. Newton[1], K. Johnston[2]

[1] Department of Physics, University of Warwick, Gibbet Hill Road, Coventry CV4 7AL, United Kingdom
[2] CERN, CH-1211 Geneva, Switzerland

Spokesperson(s): B. L. Green (b.green@warwick.ac.uk)
Local contact: Karl Johnston (karl.johnston@cern.ch)

CERN-INTC-2018-009 / INTC-P-540
10/01/2018

Abstract

The nitrogen-vacancy (NV) point defect center in diamond has recently received significant research interest, with over 850 papers published on the topic in the last 10 years. This interest is a result of optically-pumped spin polarization and optical readout of spin state with high fidelity: potential applications include high-spatial resolution magnetometry, quantum computing and quantum communications. Despite its favorable spin properties, the NV emission is highly broadband leading to low efficiencies for processes which require coherent light interactions e.g. photonic entanglement - a requirement for long distance quantum communication and distributed quantum computing. Further work in diamond has identified group-IV-vacancy pairs (SiV, GeV, SnV) with superlative optical properties (up to 70% coherent emission) but poor spin properties. Therefore, further work is required to identify a point defect which simultaneously possesses long spin lifetimes and narrow optical emission. We propose a route to the production of the previously-unidentified phosphorus-vacancy (PV) via implantation of ^{31}Al (decays to ^{31}Si with 98.4% efficiency and $t_{1/2}$ = 644 ms), and its optical identification through monitoring the decay of ^{31}SiV to ^{31}PV with $t_{1/2}$ = 157 min, and the rise of PV by photoluminescence. PV will subsequently be studied using both ensemble and single-center-capable state-of-the-art characterization equipment to determine its optical and spin properties, which we expect to be extremely interesting in line with SiV, GeV, SnV and NV in diamond.

Requested shifts: 6 shifts, (split into 2 runs over 1 years)

1 INTRODUCTION

The advent of modern telecommunications has enabled the Information Age, with remote connections between entities now a critical part of economic and social infrastructure. The ubiquity of these links has created a global need for communication security technologies, with wide-reaching implications on trust at a state and personal level. The development and implementation of quantum communications enables the possibility of deterministically secure links between remote nodes, re-establishing trust in secure communications. The long-term success of quantum communications will require the ability to communicate quantum states between different components.

Color centers in diamond currently receive a great deal of interest in the quantum communications / technologies fields due to their exceptional optical and spin properties. The negatively-charged nitrogen-vacancy center (NV^-), formed of a substitutional nitrogen atom nearest-neighbor to a lattice vacancy, is one of the most promising functional units for quantum technologies, where it has been employed for a variety of quantum entanglement, teleportation, and Bell inequality experiments [1–3] as well as applications such as hard drive quality control [4] and magnetic measurement of biological action potentials [5]. These applications stem from the rare combination of long spin lifetimes (>100 μs at room temperature) and optically-accessible spin states with high-fidelity spin initialization and readout – see Figure 1.

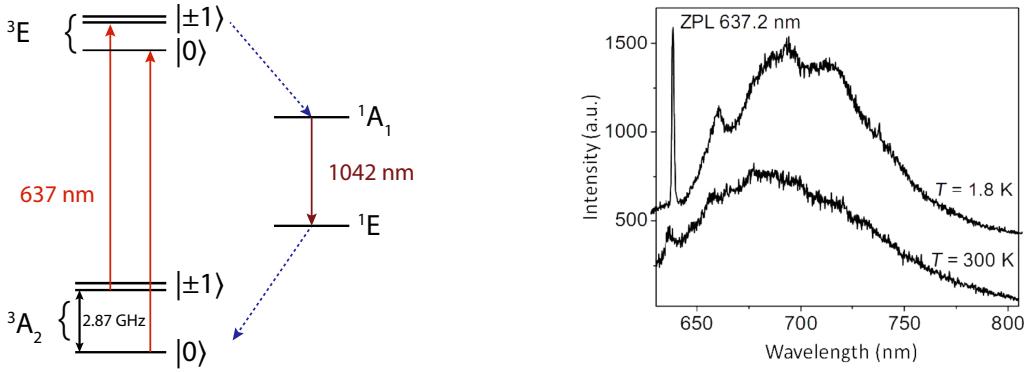

Figure 1: (Left) The relevant energy level structure for the negatively-charged nitrogen-vacancy center (NV^-). Incident optical excitation (from ~500 – 630 nm) excites electrons from the ground $^3A_2$ state to the ^3E state (a spin-conserving transition). Within the excited state, there is a spin-dependent intersystem-crossing route into the spin-singlet manifold ($^1A_1$, ^1E), which preferentially populates the ground-state m_S=0 level. This mechanism gives both high-fidelity optical spin initialization (>99% after ~300 ns) and high-contrast spin readout (approximately 30% contrast between the m_S=0 and m_S=±1 states at room temperature) [6]. (Right) Typical emission spectra from NV^- at room temperature and at 1.8 K [7]. Only approximately 3% of its emission is into the zero-phonon line at 637 nm, drastically reducing the efficiency of any entanglement schemes which rely on indistinguishable photons.

Despite its success, NV^- has two significant drawbacks for applications which require coherent spin-photon interfaces (such as long-distance quantum communication): only 3% of its emission is into the zero-phonon line (ZPL) [6]; and it is highly sensitive to electric fields caused by local strain [8]. These drawbacks have motivated the search for alternative point defects in diamond which combine the spin properties of NV^- with a narrower emission

spectrum. There is significant research into the group-IV-vacancy (G4V) complexes, with work on $SiV^{-/0}$ [9,10], GeV^- [11], and SnV^- [12] underway [Figure 2]. These defects have superlative optical properties (>70% of light emitted into the ZPL) but typically poor spin properties (e.g. SiV^- with T_2 ~ 250 ns at 3.5 K [13]). A wider search for a defect which combines the spin properties of NV^- with the optical properties of the G4V complexes is therefore highly topical and has the potential for significant impact in academic and future quantum technology industries: diamond's high Debye temperature, spin-quiet and optically transparent lattice make it the ideal host matrix for further point defect exploration and characterization.

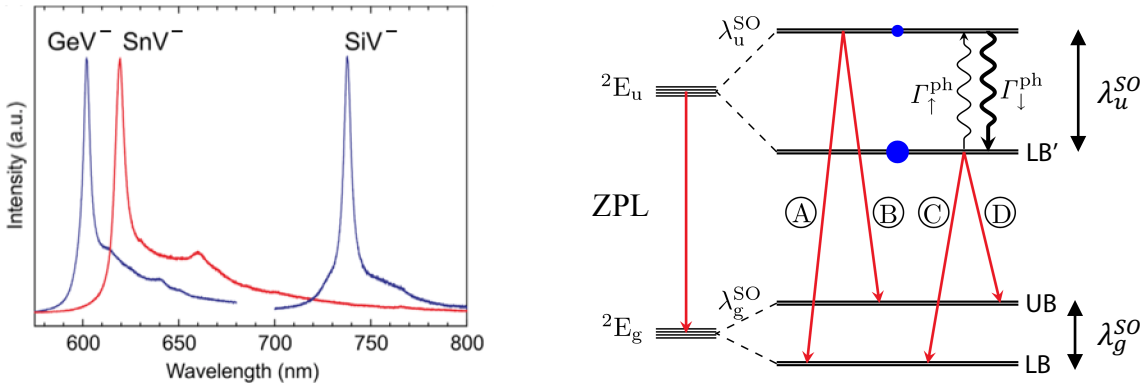

Figure 2: (Left) Room-temperature emission from negatively-charged group-IV-vacancy (G4V) point defects in diamond [12]. In all cases, the percentage of light emitted into the zero-phonon line is significantly higher than in the case of NV^-. (Right) Energy level structure common to the G4V defects (adapted from [9]). In each case, the S=1/2 ground and excited states are split by the spin-orbit interaction, with orbital lifetimes due to inter-branch phonon processes forming an upper limit to spin-lifetimes at moderate (>1 K) temperatures. Qubit schemes typically apply a magnetic field to Zeeman-split one of the orbital branches, and use optical pumping for initialization and readout.

2 THE CREATION OF PHOSPHORUS VACANCY

Phosphorus in diamond is a shallow donor, with an ionization energy of approximately 0.6 eV [14], and it has therefore attracted attention for potential use in diamond-based electronics, with several groups attempting high doping levels via chemical vapor deposition (CVD) growth [15–17]. We might expect this to produce an appreciable population of phosphorus vacancy (PV) centers, as found in CVD growth of nitrogen-doped diamond, where the ratio of N:NV is approximately 300:1 [18]. However, substitutional phosphorus is a shallow donor, and PV^0 is a deep acceptor [19]: in this material we therefore expect to find only PV^-, which is anticipated to be optically inactive by group theoretical arguments [19]. Implantation of phosphorus suffers the same problem: substitutional phosphorus and PV complexes undergo mutual charge compensation i.e. $P^0 + PV^0 \rightarrow P^+ + PV^-$.

To date, there is no optical signature associated with either PV^0 or PV^+ - given the similarity of this defect to both the G4V and NV^-/SiV^0 defects, it is an ideal candidate for study to characterize its optical and spin properties. We anticipate PV^0 will possess electronic structure similar to the negatively-charged G4V defects (S=1/2), and PV^+ to be electronically similar to SiV0 (S=1). Thus, we expect both charge states to possess methods for optical spin initialization and readout, with high fraction of emission into the ZPL due to inversion

symmetry as seen in the G4V defects. Additionally, only ^{31}P is stable, giving 100% of created defects an additional quantum memory resource in the form of the I=1/2 nuclear spin.

However, many point defects in diamond are luminescent: to concentrate on only those luminescence lines associated with phosphorus, we propose the production of PV via the implantation and subsequent decay of ^{31}Al. We believe this is the only way to reliably produce and identify PV. The implantation will leave aluminum in interstitial and substitutional sites in addition to creating intrinsic lattice damage in the form of vacancies and self-interstitials. ^{31}Al decays with 98.4% efficiency to ^{31}Si with $t_{1/2}$ = 644 ms. Upon annealing at temperatures of 800 °C and above the intrinsic vacancies become mobile, forming SiV$^{0/-}$: the neutral and negative charge states of SiV emit at 946 and 737 nm, respectively [10,20], and can be easily monitored using the cryogenic PL facilities at ISOLDE. In turn, the ^{31}SiV will decay to ^{31}PV with $t_{1/2}$ = 157.3 min: we therefore expect to see the SiV signals decay with the characteristic ^{31}Si lifetime, accompanied by increases in optical lines associated with PV$^{+/0}$ with the same lifetime [see Figure 3]. As a previously-unidentified defect, we expect the identification and characterization of PV$^{+/0}$ in diamond to stimulate significant interest in the field and to be published in world-leading journals.

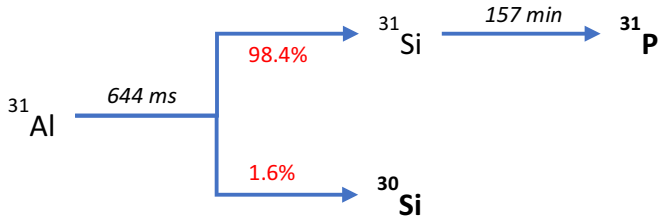

Figure 3: Decay pathways from ^{31}Al, with stable isotopes given in bold and half-lives given in italics.

3 IN-DEPTH PROPOSAL

3.1 Ion doses and characterization plan

An acceleration energy of 50 keV corresponds to an implant depth of approximately 50±15 nm in diamond. Shallow implants are problematic in investigations of shallow NV$^-$ and SiV$^-$ defects, where the surface typically acts to passivate the defects to their neutral charge states, but is advantageous in our study where we are targeting the neutral and positive charge states of PV.

With an ion flux of approximately 2×10^9 ions/hr in a beam size of 2x2 mm^2, we will require approximately 2 hours to reach a dose of 10^{11} ions/cm^2. Typical yields are approximately 1% for the conversion of implanted silicon to silicon vacancy [12], resulting in an anticipated 100 SiV defects per square micron: using the high-sensitivity, cooled CCD and InGaAs detectors available at ISOLDE, this will provide a very high signal-to-noise ratio for subsequently monitoring the decay of ^{31}SiV to ^{31}PV. The experimental plan for a high-dose run, including timings in multiples of ^{31}Si half-lives, is given in Table 1.

In addition to high-dose implantation runs for ensemble measurements, we will also prepare samples with a low-dose for final expected concentrations of less than one defect per square micron [Table 2]. These samples will be taken back to Warwick for characterization using our state-of-the-art laser-scanning confocal microscopes, which are capable of interrogating and

characterizing single point defects at both room temperature and under cryogenic conditions. We will therefore be in a position to characterize both the ensemble and single-center characteristics of PV for a holistic view of the defects' physical properties.

Table 1: Timings for a high-dose (1×10^{11} ions/cm^2) implantation run. PL measurements should begin with approximately 25% of initial ^{31}Si population remaining for the highest-dose runs; lower-dose runs will begin up to an hour earlier via reduced implantation times.

Time (hh:mm)	No. ^{31}Si half-lives	Stage	Notes
00:00	0	Implantation of ^{31}Al	Decays to Si with $t_{1/2}$<1 s
02:30	1.0	Insertion into furnace	Furnace at 850°C to create SiV
04:30	1.7	Removal from furnace	^{31}SiV decaying to ^{31}PV
05:00	1.9	Insertion into cryostat	Cryostat pre-cooled to 100 K
05:30	2.1	PL measurements begin	Monitor decrease/increase of PL lines

Table 2: Planned runs of different doses with associated run-times, and number of repeated runs per dose. Initial experimental runs will focus on the high-dose samples for the highest probability of detecting PV. Each of the runs will be performed at least once on each of an intrinsic a p-type sample to maximize the chances of detecting the neutral and positive charge states. As the PL measurements are to be performed immediately after the implantation, the planned runs will be re-assessed during the allotted time to maximize the output of the beamtime.

Dose (ions/cm^2)	Implantation time (hh:mm)	Repeats	Notes
1×10^{9}	0:02	2	Low density will allow optical addressing of single defects
3×10^{9}	0:04	2	
1×10^{10}	0:12	2	
5×10^{10}	1:00	2	High density to produce ensembles for initial detection
1×10^{11}	2:00	4	

3.2 Samples

Samples for the project will be donated by our industrial partners, Element Six Ltd., and will consist of both high-purity (intrinsic) material and boron-doped (p-type) material. This will ensure we are able to maintain either a neutral or positive charge state of PV, as opposed to the optically inactive negative state. The surfaces of each sample will be prepared using proprietary techniques developed in partnership between Warwick and Element Six, and which have been shown to produce extremely low sub-surface damage and hence maximize the quantum properties of near-surface defects. All samples will be prepared on both sides and laser-marked to enable implantation into both surfaces.

4 ADVANCE PREPARATION

Due to the relatively short half-life of ^{31}Si, the success of this proposal will depend on high-quality photoluminescence collection and correctly-operating optically-accessible cryogenic

equipment. We have agreed with our local ISOLDE contact (Karl Johnston) that two researchers from Warwick will spend 3-4 days at ISOLDE in advance of the allocated beamtime in order to optimize the PL systems for collection from diamond. As diamond is a wide-band-gap semiconductor, we wish to maximize the wavelength range over which we can search for PV: we will therefore bring samples which strongly luminesce when excited at 442/325 nm, 532 nm, ~800 nm and 1064 nm to optimize the optics at each wavelength. This will allow us to identify any additional optics required and to purchase them if necessary.

5 BEAM REQUEST

The production of ^{31}Al is typically of the level of 2.5e5 ions/uC for a UCx target with the RILIS ion source [21]. This results in about 5e5 ions per second for 2uA of proton beam. Al can also be well produced with a W ion source or Re ion source. As such the proposed experiments could be accommodated either within a dedicated Al run or as part of a larger run utilizing a surface ion source. The request is for 6 shifts of radioactive beam in total which would allow for 2 separate runs in 2018 (if required), although the physics goals could be conceivably achieved in less time under optimal conditions.

6 CONCLUSION

Through a combination of the advance preparation described above, the preparation and implantation of multiple (p-type and intrinsic) samples, and the fast feedback provided by a <1 day implantation and measurement cycle, we believe this proposal will be successful in the identification and characterization of PV, with subsequent publication in world-leading journals.

7 REFERENCES

[1] H. Bernien et al., Nature **497**, 86 (2013).
[2] W. Pfaff et al., Science **345**, (2014).
[3] B. Hensen et al., Nature **526**, 682 (2015).
[4] I. Jakobi et al., Nat. Nanotechnol. **12**, 67 (2017).
[5] J. F. Barry et al., Proc. Natl. Acad. Sci. **113**, 14133 (2016).
[6] M. W. Doherty et al., Phys. Rep. **528**, 1 (2013).
[7] K. Beha et al., Beilstein J. Nanotechnol. **3**, 895 (2012).
[8] Y.-C. Chen et al., Nat. Photonics **11**, 77 (2017).
[9] B. Pingault et al., Nat. Commun. **8**, 15579 (2017).
[10] B. L. Green et al., Phys. Rev. Lett. **119**, 96402 (2017).
[11] T. Iwasaki et al., Sci. Rep. **5**, 12882 (2015).
[12] T. Iwasaki et al., Phys. Rev. Lett. **119**, 253601 (2017).
[13] D. D. Sukachev et al., Phys. Rev. Lett. **119**, 223602 (2017).
[14] M. A. Pinault-Thaury et al., Appl. Phys. Lett. **100**, 192109 (2012).
[15] W. Janssen et al., Phys. Status Solidi - Rapid Res. Lett. **8**, 705 (2014).
[16] M. A. Pinault-Thaury et al., Phys. Status Solidi Appl. Mater. Sci. **212**, 2454 (2015).
[17] Y. Balasubramaniam et al., Appl. Phys. Lett. **109**, 62105 (2016).
[18] A. M. Edmonds et al., Phys. Rev. B **86**, 35201 (2012).
[19] R. Jones et al., Appl. Phys. Lett. **69**, 2489 (1996).
[20] L. J. Rogers et al., Phys. Rev. B **89**, (2014).
[21] https://isoyields2.web.cern.ch/YieldByElement_Detail.aspx?Z=13 (2018).

Appendix

8 DESCRIPTION OF THE PROPOSED EXPERIMENT

The experimental setup comprises: SSP GLM or SSP GHM, plus characterization facilities available at ISOLDE (cryogenic photoluminescence).

Part of the experiment	Availability	Design and manufacturing
SSP GLM or SSP GHM to implant ^{31}Al	☒ Existing	☒ To be used without any modification
PL lab in building 508	☒ Existing	☐ To be used without any modification ☐ To be modified
	☐ New	☐ Standard equipment supplied by a manufacturer ☐ CERN/collaboration responsible for the design and/or manufacturing
[Part 2 experiment/ equipment]	☐ Existing	☐ To be used without any modification ☐ To be modified
	☐ New	☐ Standard equipment supplied by a manufacturer ☐ CERN/collaboration responsible for the design and/or manufacturing
[insert lines if needed]		

9 HAZARDS GENERATED BY THE EXPERIMENT

Hazards named in the document relevant for the fixed SSP-GLM or SSP-GHM chamber installation.

Additional hazards:

Hazards			
	Implantation of ^{31}Al	***PL lab in building 508***	*[Part 3 of the experiment/equipment]*
Thermodynamic and fluidic			
Pressure			

Vacuum		Cryostat vacuum	
Temperature		4-300 K	
Heat transfer			
Thermal properties of materials			
Cryogenic fluid		Liquid helium, 30-60 l	
Electrical and electromagnetic			
Electricity			
Static electricity			
Magnetic field			
Batteries	☐		
Capacitors	☐		
Ionizing radiation			
Target material	Diamond		
Beam particle type (e, p, ions, etc)	Ions		
Beam intensity			
Beam energy	50 keV		
Cooling liquids		Liquid helium	
Gases		Helium exchange	
Calibration sources:	☐		
• Open source	☒		
• Sealed source	☐ [ISO standard]		
• Isotope	31Si		
• Activity	73 kBq		
Use of activated material:			
• Description	☐		
• Dose rate on contact and in 10 cm distance	1e-4 mSV	1e-4 mSV	
• Isotope			
• Activity			
Non-ionizing radiation			
Laser		325nm @ 50mW, 442 nm @ 50 mW, 1064 nm @ 50 mW	
UV light			
Microwaves (300MHz-30 GHz)			
Radiofrequency (1-300MHz)			
Chemical			
Toxic			
Harmful			
CMR (carcinogens, mutagens and substances toxic to reproduction)			
Corrosive			
Irritant			
Flammable			
Oxidizing			
Explosiveness			
Asphyxiant			
Dangerous for the environment			
Mechanical			

Physical impact or mechanical energy (moving parts)			
Mechanical properties (Sharp, rough, slippery)			
Vibration			
Vehicles and Means of Transport			
Noise			
Frequency			
Intensity			
Physical			
Confined spaces			
High workplaces			
Access to high workplaces			
Obstructions in passageways			
Manual handling			
Poor ergonomics			

9.1 Hazard identification

9.1.1 Average electrical power requirements

N/A